Eur. Phys. J. D **20**, 403–408 (2002)
DOI: 10.1140/epjd/e2002-00143-x

THE EUROPEAN PHYSICAL JOURNAL D

Stimulated Raman spectroscopic study on intermolecular vibrations of size-selected benzonitrile clusters

R. Yamamoto, T. Ebata[a], and N. Mikami

Department of Chemistry, Graduate School of Science, Tohoku University, Sendai 980-8578, Japan

Received 28 April 2002 / Received in final form 30 May 2002
Published online 13 September 2002 –

Abstract. Low frequency intermolecular vibrations of benzonitrile-$(H_2O)_{n=1-3}$, -$(CH_3OH)_{n=1-3}$, and -$(CHCl_3)_{n=1-3}$ clusters were observed by stimulated Raman – UV double resonance spectroscopy combined with fluorescence detection. The Raman active vibrations, which appear in the region from 5 to 50 cm^{-1}, exhibit characteristic frequency shifts depending on the cluster structure and on the cluster size. In benzonitrile-$(H_2O)_{n=1-3}$ and -$(CH_3OH)_{n=1-3}$, the lowest frequency band showed a lower frequency shift with an increase of the number of solvent molecules. On the other hand, that of benzonitrile-$(CHCl_3)_{n=1-3}$ showed a shift to the higher frequency side. Their characteristic shifts are discussed based on the structure of the clusters.

PACS. 34.30.+h Intramolecular energy transfer; intramolecular dynamics; dynamics of van der Waals molecules – 36.40.Mr Spectroscopy and geometrical structure of clusters – 39.30.+w Spectroscopic techniques

1 Introduction

Structure and dynamics of molecular clusters formed in supersonic jets have long been investigated as ideal systems for understanding solute-solvent interactions of condense phases. Among many spectroscopic information on the clusters, vibrational spectroscopy dealing with the characteristic frequency shifts upon the cluster formation is very useful, since the shifts are directly connected to the geometry and intermolecular potential of the clusters. For this purpose, our group has been applying infrared (IR) and stimulated Raman – UV double resonance spectroscopic methods to the measurement of the vibrational spectra of jet-cooled clusters [1–4]. Especially, for the hydrogen-bonded clusters, IR spectroscopy in the OH stretching vibrational region combined with *ab initio* molecular orbital (MO) calculations is demonstrated to be quite powerful for unambiguous structural determination of H-bonded networks [1,2].

An investigation of intermolecular vibrations of clusters is also very important to determine the cluster structure. Furthermore, the intermolecular vibrations play an important role as bath modes in the intracluster vibrational energy redistribution (IVR). In general, the electronic transition has been widely used for the observation of the intermolecular vibrations of clusters involving aromatic molecule. However, if the change along the vibrational coordinate of interest is small between S_1 and S_0, the vibration is hardly observed due to poor Franck-Condon factors. Another method to observe the intermolecular vibrations is vibrational spectroscopy. Especially, Raman spectroscopy has been used for the investigation of vibrations in the low frequency region [5,6] Recently, Felker and coworkers used stimulated Raman-UV double resonance spectroscopy with an ionization detection to observe the intermolecular vibrations of size-selected clusters [7–12].

In this work, we present the observation of the intermolecular vibrations of benzonitrile-$(H_2O)_{n=1-3}$, -$(CH_3OH)_{n=1-3}$, and -$(CHCl_3)_{n=1-3}$ clusters by fluorescence detected stimulated Raman spectroscopy (FDSRS). Our goal is the characterization of the relationship between the cluster structures and the intermolecular vibrations. We have been investigating the structures and the vibrational relaxation of the clusters of benzonitrile (BN) by stimulated Raman – UV double resonance spectroscopy with fluorescence detection, so-called fluorescence detected stimulated Raman spectroscopy (FDSRS) [2–4]. In parallel, we carried out *ab initio* MO calculations and determined the cluster structure which reproduces the observed vibrational spectra. Figure 1a shows the structures of BN-$(H_2O)_{n=1-3}$ determined by such the manner. They are the *ab initio* calculated most stable structures at HF/6-31G(d,p) level, and we found that the simulated vibrational spectra of each structure reproduced well the experimentally observed ones. Furthermore, the structure of BN-$(H_2O)_1$ is precisely determined by high resolution UV and microwave spectroscopy [13–15], which agrees with

[a] e-mail: ebata@qclhp.chem.tohoku.ac.jp

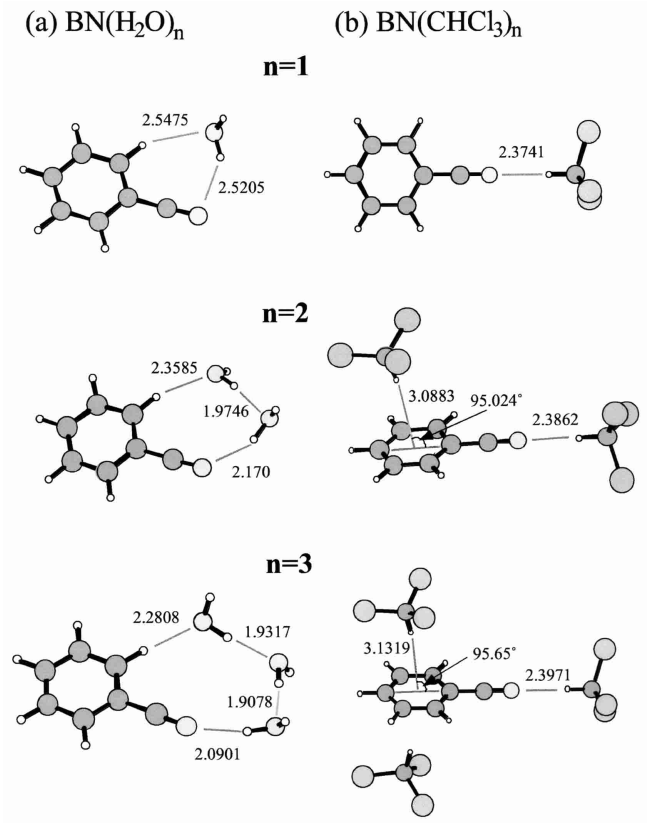

Fig. 1. The structures of (a) benzonitrile-$(H_2O)_{n=1-3}$ obtained at HF/6-31G(d,p) level calculation and (b) benzonitrile-$(CHCl_3)_{n=1-3}$ obtained at HF/6-31+G(d,p) level calculation. The inter-atomic distances (Å) and angles (deg) are also shown. The figures are drawn using the MOLCAT program [21].

that shown in Figure 1a. The cluster with $n = 1$ has the "side type" structure, where H_2O is H-bonded to the CN group and to the ortho C–H of BN. The clusters with $n = 2$ and 3 have the "ring type" structures, where the chain-formed water cluster is H-bonded to the ortho C-H and to the CN group of BN. BN-$(CH_3OH)_{n=1-3}$ also have the very similar structures as BN-$(H_2O)_{n=1-3}$ [2].

Figure 1b shows the *ab initio* calculated most stable structures of BN-$(CHCl_3)_{n=1-3}$ at HF/6-31+G(d,p) level. Their structures have been also confirmed by high resolution UV spectroscopy and by double resonance vibrational spectroscopy in our previous work [4]. The cluster with $n = 1$ has the "linear type" structure, where the CH hydrogen of $CHCl_3$ is H-bonded linearly to the N end of the CN group of BN. The clusters with $n = 2$ and 3 form the "shell type" structures, where the second and third $CHCl_3$ molecules are H-bonded to the phenyl ring of BN. Thus, we can classify the structures of the H-bonded BN clusters into two types, that is, "ring type" and "shell type". We expect that the intermolecular vibrations will exhibit the vibrational structure reflecting such a difference between the two forms. The electronic spectra of BN clusters have been investigated in detail by several groups [2–4,16–18], and most of the spectra show very weak intermolecular bands so that the use of electronic transition is not suitable for the observation of their vibrations. Therefore, stimulated Raman–UV double resonance spectroscopy may be most appropriate to observe them and to investigate the relationship between the intermolecular vibrations and the cluster structures.

2 Experiment

Since the excitation schemes and the experimental setup of FDSRS have been reported in detail elsewhere [2–4], we briefly explain them here. In the Raman-dip measurement, the population of the zero point level ($v'' = 0$) in S_0 of a particular cluster was monitored by laser induced fluorescence (LIF) with the UV laser pulse. Two laser pulses for the stimulated Raman pumping were introduced prior to the UV pulse. The depletion of the ground state population induced by the stimulated Raman pumping resulted in a decrease (dip) of the LIF intensity. Thus, a fluorescence-dip spectrum representing the Raman spectrum was obtained. We also applied Raman-enhancement measurement. In this case, the UV frequency was slightly (a few wavenumbers) detuned to the lower frequency side of the $(0, 0)$ band. Due to the slight frequency difference of the intermolecular vibrations between S_0 and S_1, the UV frequency was resonant to the $v' = 1 \leftarrow v'' = 1$ transition by the slight detuning of the frequency, and we obtained the enhancement of the LIF signal when the stimulated Raman transition occurred.

The backward scattered first Stokes light (629.86 nm) generated from a Raman shifter by the irradiation of the second harmonic of the injection seeded Nd:YAG laser (Spectra Physics GCR-230-10) was used either as the pump ($h\nu_1$) or Stokes laser light ($h\nu_2$). The Nd:YAG laser pumped dye laser (Continuum ND 6000) was used either as $h\nu_1$ or $h\nu_2$. The Raman shifter had a 50 cm length and was filled with 20 atm pressure of CH_4. The conversion efficiency of the first Stokes light was about 20% when the second harmonic of the injection seeded Nd:YAG laser was focussed by an $f = 300$ mm lens. The probe UV laser was a second harmonic of the Nd:YAG laser pumped dye laser (Spectra-Physics INDI-50/LUMONICS Hyper Dye 500). The wavelength of the dye lasers was calibrated with an optogalvanic tube, and that of the injection seeded Nd:YAG laser and the first Stokes light from the Raman shifter were calibrated by a wavemeter (Burleigh WA-4500). Their accuracy was ± 0.2 cm^{-1}. The spectral resolution of the UV laser light was 0.2 cm^{-1}. Those of second harmonic of the injection seeded Nd:YAG laser and the Nd:YAG laser pumped dye laser were 0.0015 and 0.1 cm^{-1}, respectively. The delay time between the stimulated Raman pumping and the probe UV laser pulses was controlled with a digital pulse generator (Stanford Research Systems DG 535) and the typical delay time was 30 ns. Fluorescence was detected with a photomultiplier tube (Hamamatsu Photonics R166UH) after passing through a band pass filter (New Lambda Corporation UG-11). The photocurrent was integrated by a boxcar

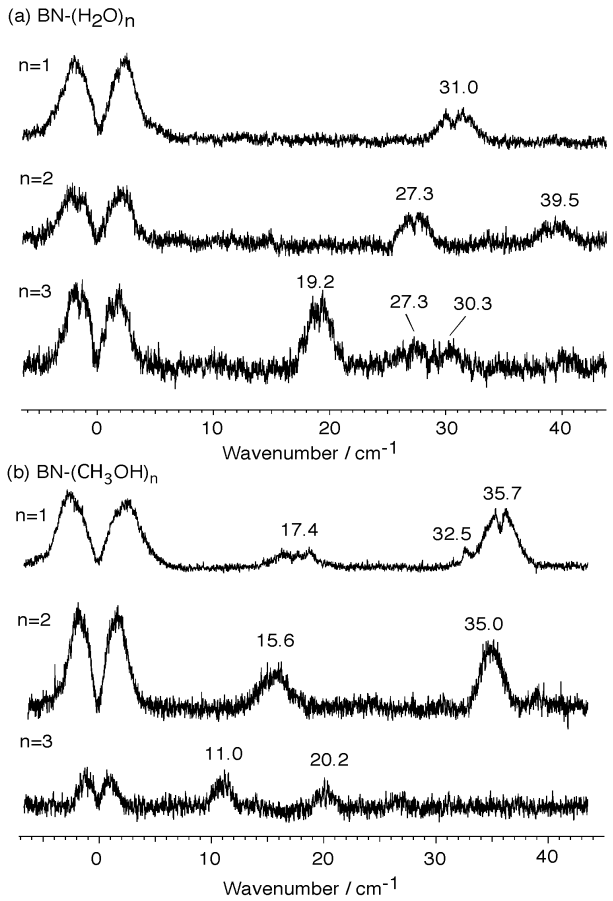

Fig. 2. Fluorescence-enhancement stimulated Raman spectra of (a) benzonitrile-$(H_2O)_{n=1-3}$ and (b) benzonitrile-$(CH_3OH)_{n=1-3}$ in the intermolecular vibrational region.

integrator (Par Model 4400) which was connected to a personal computer.

The jet-cooled BN and its clusters were generated by a supersonic expansion of a gaseous mixture of benzonitrile and solvents seeded with He carrier gas through a nozzle having an 800 μm orifice. The temperature of BN was kept at 330 K to obtain a sufficient vapor pressure. The vapor pressure of H_2O was that at room temperature, while those of CH_3OH and $CHCl_3$ were controlled with a thermoregulater. Benzonitrile (98%), methanol (99%), and chloroform (99%) were purchased from Kanto Chemical Co., Inc., and were used without further purification.

Ab initio MO calculations were carried out by using Gaussian 98 packaged program [19] with HF/6-31G(d,p) or HF/6-31+G(d,p) level. Fully energy optimized structures were obtained without any geometry constraint.

3 Results

Figure 2a shows the Raman-enhancement spectra of BN-$(H_2O)_{n=1-3}$ in the region from 0 to 45 cm^{-1}. We observed these spectra by detuning the UV laser frequency by 4 cm^{-1} to lower frequency side of the $(0,0)$ band. In each spectrum, an envelope due to the rotational Raman band appeared in a range from 0 to 3 cm^{-1}. In the cluster with $n = 1$, a doublet structured band appeared at 31.0 cm^{-1}. In the $n = 2$ cluster, two bands appeared at 27.3 and 39.5 cm^{-1}. For the $n = 3$ cluster, three bands were observed at 19.2, 27.3, and 30.3 cm^{-1}. We see that the band widths are about a few wavenumber, which are much wider than those of totally symmetric Raman bands reported in our previous papers [2–4]. The rather wide widths of the intermolecular Raman bands indicates that they are the non-totally symmetric vibrations and the doublet feature is attributed to the rotational contour. This is because that the Raman band of the totally symmetric vibration mainly consists of the Q-branch, while in the nontotally symmetric vibration, P and R branches have considerable intensities. Recently, Felker and coworker analyzed the rotational contour of the intermolecular Raman bands by using a pendular model [10–12]. The estimated laser power in the present work was 1.5 MW/cm^2, which is a lower limit of their experimental condition. In this sense, a similar treatment can be applied. However, since the observed Raman bands shown in Figure 2a do not show distinct rotational structures, which may be due to low symmetry of the clusters and small rotational constants, we have not carried out further analysis.

We also observed the Raman-dip spectra for BN-$(H_2O)_{n=1-3}$, which are essentially the same with the Raman-enhanced spectra. The percentage of the depletion was 30% for the rotational Raman bands and 10∼15% for the intermolecular bands, so that the S/N ratio was not good enough to identify weak bands which were observed in the Raman-enhancement spectra. For other bands in the higher energy region of 45–150 cm^{-1}, we could not observe any bands despite of the careful examination by the Raman-dip and Raman-enhancement measurements.

Figure 2b shows the Raman-enhancement spectra for BN-$(CH_3OH)_{n=1-3}$ in the region from 0 to 45 cm^{-1}. In the $n = 1$ cluster, three intermolecular bands are observed at 17.4, 32.5, and 35.7 cm^{-1}. It is seen that the Raman spectrum of BN-$(CH_3OH)_1$ shows more vibrational bands than that of BN-$(H_2O)_1$. For the $n = 2$ cluster, two vibrational bands appeared at 15.6 and 35.0 cm^{-1}. For the $n = 3$ cluster, two bands appeared at 11.0 and 20.2 cm^{-1}. Similar to BN-$(H_2O)_{n=1-3}$, the bands in the 45 to 150 cm^{-1} region were too weak to be identified in BN-$(CH_3OH)_{n=1-3}$.

Figure 3 shows the Raman-dip spectra of the intermolecular vibrations of BN-$(CHCl_3)_{n=1-3}$ in the region from 0 to 35 cm^{-1}. In contrast to BN-$(H_2O)_1$ and -$(CH_3OH)_1$, very low frequency vibrations as low as 5.2 and 5.9 cm^{-1} were observed in the spectrum of BN-$(CHCl_3)_1$. The two vibrations are not attributed to the same mode of the isotopomers of naturally abundant $CHCl_3$, since the frequency differences of the intermolecular vibrations between BN-$CH^{35}Cl_3$ and BN-$CH^{37}Cl_3$ are roughly estimated to be 2∼3%. The percentage of the depletion of these vibration were 50%. BN-$(CHCl_3)_1$ exhibits another vibration at 11.7 cm^{-1}, whose frequency is close to that of the overtone of the lowest vibration.

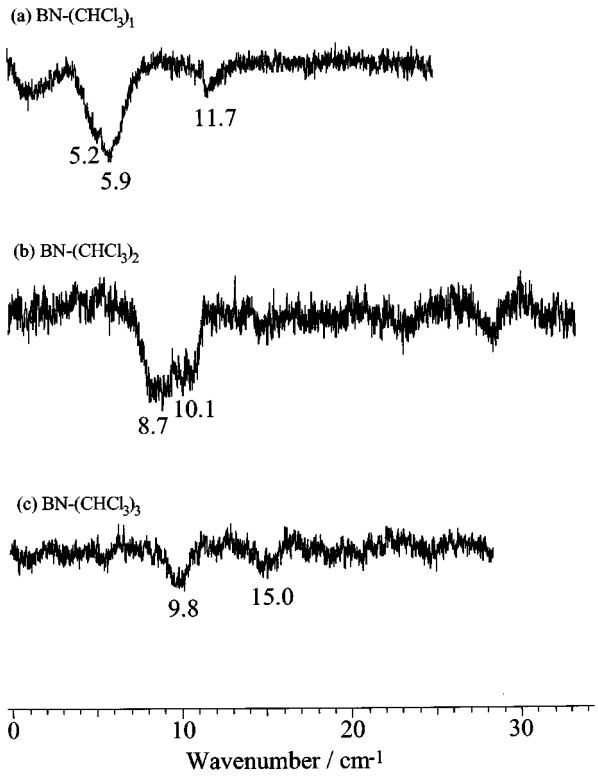

Fig. 3. Fluorescence-dip stimulated Raman spectra of benzonitrile-$(CHCl_3)_{n=1-3}$ in the intermolecular vibration region.

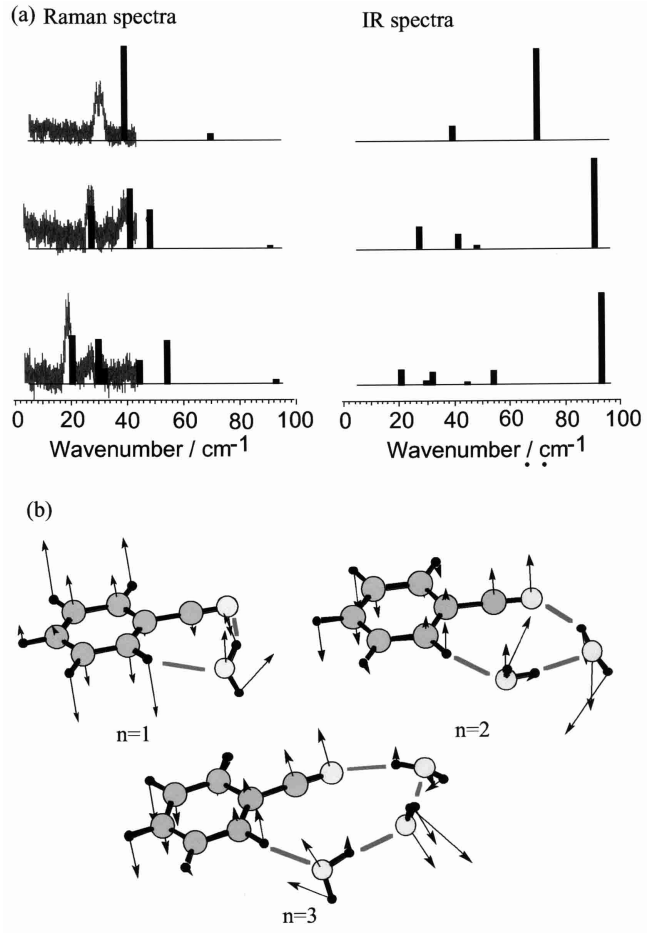

Fig. 4. (a) Calculated Raman and IR spectra (bar graph) of intermolecular vibrations of the benzonitrile-$(H_2O)_{n=1-3}$ clusters shown in Figure 1. The observed Raman spectra are also shown with hatched curves. (b) The calculated normal modes of the lowest frequency vibrations of benzonitrile-$(H_2O)_{n=1-3}$ at the HF/6-31G(d,p) level.

However, this assignment is quite unlikely because the $\Delta v = 2$ Raman transition is normally very weak, and this band should be assigned to the fundamental of other intermolecular vibration. The $n = 2$ cluster shows overlapped bands at $\sim$10 cm^{-1}, which consists of a main peak at 8.7 cm^{-1} and a weaker one at 10.1 cm^{-1}. The $n = 3$ cluster shows two vibrations at 9.8 and 15.0 cm^{-1}. In the frequency region higher than 30 cm^{-1}, no vibration was observed in each cluster.

4 Discussion

The normal mode analyses of the intermolecular vibrations were carried out on the basis of the *ab initio* calculation at HF/6-31G(d,p) or HF/6-31+G(d,p) level. Figure 4a shows the simulated Raman and IR spectra of BN-$(H_2O)_{n=1-3}$ in the region from 0 to 100 cm^{-1}. The observed Raman spectra are also shown for comparison. Table 1 lists the calculated vibrational frequencies, reduced masses, force constants, IR intensities, and Raman activities for the intermolecular vibrations. As shown in the figure, several features are seen in the calculated Raman and IR bands. First, in the calculated spectra most of the Raman active bands appear below 50 cm^{-1}, which agrees with our observations. Second, most of the Raman active vibrations are weak in the IR spectra, while strong IR vibrations appear in the region above 60 cm^{-1}. Thus, there is a clear intensity alternation between the Raman and the IR spectra, and the calculations support the observation that the Raman active vibrational bands should appear below 60 cm^{-1}. Finally, we see that in the calculated spectra the lowest frequency vibration shifts to the lower frequency side with the increase of the cluster size, which also agrees well with the observed tendency. Figure 4b shows the vector model of the lowest frequency modes of BN-$(H_2O)_{n=1-3}$. As seen in the figure, these modes include the non-totally symmetric out-of-plane rocking motion of BN. The result agrees well with the relatively wide bandwidth of the observed Raman bands as discussed previously. The similar tendency, that is the out-of-plane motion of phenyl ring has a large Raman intensity, has been also found in the benzene clusters [6].

For BN-$(CH_3OH)_{n=1-3}$, though the low frequency motion of the methyl group of methanol is thought to cause the complexity of intermolecular vibrational mode, the obtained Raman spectra show a simple feature. We also simulated the Raman spectra for BN-$(CH_3OH)_{n=1-3}$ at the HF/6-31(d,p) level. However, they were not good enough

Table 1. Vibrational frequencies (cm^{-1}) observed in the work. Frequency (cm^{-1}), reduced mass (amu), force constants (mDyne/A), IR intensity (km/mole), and Raman activity ($Å^4$/a.m.u) of intermolecular vibrations of BN-$(H_2O)_{n=1-3}$ in the low frequency region, which are obtained by *ab initio* MO calculations with HF/6-31G(d,p) level.

cluster	obs. freq. (cm^{-1})	calc. freq. (cm^{-1})	red. mass (amu)	force const. (mDyne/A)	IR intensity (km/mole)	Raman activity ($Å^4$/amu)	the motion of BN
BN-$(H_2O)_1$	31.0	39.7	4.2244	0.0039	1.5918	6.8339	out-of-plane
		70.2	6.7885	0.0197	10.3665	0.3933	in-plane
BN-$(H_2O)_2$	27.3	27.5	6.0474	0.0027	2.4733	2.9893	out-of-plane
	39.5	41.6	4.4090	0.0045	1.6284	4.2270	out-of-plane
		48.3	5.2891	0.0073	0.3133	2.7213	out-of-plane
		90.9	7.2595	0.0354	10.1857	0.1396	in-plane
BN-$(H_2O)_3$	19.2	20.6	5.7809	0.0014	1.7001	3.5042	out-of-plane
	27.3	29.8	4.7427	0.0025	0.4841	3.2583	out-of-plane
	30.3	32.0	6.3130	0.0038	1.4506	1.0384	in-plane
		44.6	5.8281	0.0068	0.3033	1.6740	out-of-plane
		54.1	4.9832	0.0086	1.6275	3.1246	out-of-plane
		93.0	6.8642	0.0350	10.3513	0.2143	in-plane

to reproduce the observed Raman spectra. In spite of the disagreement between the observed and calculated spectra, we can safely guess that the vibrational bands in the Raman spectra involve the out-of-plane rocking motion of BN similar to those of BN-$(H_2O)_{n=1-3}$. As seen in Figure 2b, we see that the lowest frequency Raman band shifts to lower frequency side with the size of the cluster. Thus, we can conclude that the frequency of out-of-plane rocking motion of BN decrease with an increase of the size of ring-type cluster.

For BN-$(CHCl_3)_{n=1-3}$, the simulated Raman spectra with the HF/6-31+G(d,p) level calculation did not give a satisfactory agreement with the observed ones. However, from the fact that the rotational band and the vibrations which involve the out-of-plane motion of BN has Raman activities in BN-$(H_2O)_n$ and -$(CH_3OH)_n$, the observed intermolecular Raman bands of BN-$(CHCl_3)_n$ can be also thought to be the vibrations involving the out-of-plane motion of BN.

Finally, we discuss the relationship between the cluster structures and the intermolecular Raman bands. As was shown previously, BN-$(H_2O)_{n=1-3}$ exhibits the "ring type" structure and the lowest frequency Raman band shows a lower frequency shift with an increase of the number of the solvent molecules. In order to discuss such a tendency of the shift of the Raman band, we compare them with the Raman spectra of other aromatic-$(H_2O)_n$ system. Among the aromatic-$(H_2O)_n$ clusters investigated, benzene-$(H_2O)_{n=1-5}$ are most appropriate for the comparison with BN-$(H_2O)_{n=1-3}$. Maxton *et al.* has observed the intermolecular Raman spectra of benzene-$(H_2O)_{n=1-5}$ [7]. They reported that the Raman bands of benzene-$(H_2O)_{n=1-5}$ appeared in the range of 35–65 cm^{-1}, whose frequencies were higher than those of BN-$(H_2O)_{n=1-3}$. In addition, their band positions were almost invariant irrespective of the cluster size. Benzene-$(H_2O)_{n=1-5}$ have the "on top" structure, where the water clusters located above the benzene ring, being H-bonded to the π-electron of the benzene ring [20]. In this case, the out-of-plane motion of benzene molecule may be insensitive to the size or structure of water cluster. On the other hand, as was shown above, the Raman active intermolecular bands of BN-$(H_2O)_{n=1-3}$ appeared below 50 cm^{-1}, and the lowest frequency band showed a red-shit with an increase of n. The differences in the band positions and frequency shift between benzene-$(H_2O)_n$ and BN-$(H_2O)_n$ are thought to be due to the difference in their structures. The observed decrease of the frequency of the rocking motion of BN with the size indicates either the increase of the reduced mass of this motion or the reduction of force constant. As seen in Table 1, *ab initio* MO calculations show a very small change in the reduced mass but a large reduction in the force constant for the lowest frequency vibration of BN-$(H_2O)_n$ with the increase of n. These results indicate that the H-bond network structure becomes more flexible with the increase of the size so that BN can easily librate along the out-of-plane in the larger size clusters. The same tendency observed in BN-$(CH_3OH)_n$ can be explained by the same manner since the clusters also have the "ring type" structure.

Different from BN-$(H_2O)_n$ and -$(CH_3OH)_n$, the lowest frequency bands of BN-$(CHCl_3)_{n=1-3}$ shifted to the higher frequency side with an increase of the number of the solvent molecules. Since $CHCl_3$ is located at the N end of BN in BN-$(CHCl_3)_1$, the torsional motion of BN about the intermolecular axis should have a large Raman intensity with a very low frequency, as was observed. In BN-$(CHCl_3)_{2,3}$, their structures are of "shell-type", where the second and third BN-$(H_2O)_n$ molecules locate above the phenyl ring of BN. Therefore, the second and third solvents are thought to prevent the torsional motion of BN, resulting in the higher frequency shift of this vibration. Such the band shifts with the increase of the solvent molecules show the characteristic feature of the solvent surrounded by solvents.

From these results, we can conclude that the intermolecular Raman band involving the motion of the solute molecule is the sensitive probe for the characterization of the cluster structure.

5 Conclusion

We observed Raman spectra of intermolecular vibrations for BN-$(H_2O)_{n=1-3}$, -$(CH_3OH)_{n=1-3}$, and -$(CHCl_3)_{n=1-3}$ in the 0–100 cm^{-1} region by fluorescence detected stimulated Raman spectroscopy. Fluorescence enhancement technique improved the S/N ratio of the Raman spectra of BN-$(H_2O)_{n=1-3}$ and -$(CH_3OH)_{n=1-3}$. For BN-$(H_2O)_{n=1-3}$ and -$(CH_3OH)_{n=1-3}$, most of the Raman active bands appeared in the 10–40 cm^{-1} region. For BN-$(CHCl_3)_{n=1-3}$, very low frequency bands were observed in the region from 5 to 20 cm^{-1}. *Ab initio* MO calculations of BN-$(H_2O)_{n=1-3}$ indicate that the Raman active modes are the out-of-plane motion of BN. The relationship between the cluster structures and the frequencies of the intermolecular Raman bands was obtained as follows. In BN-$(H_2O)_{n=1-3}$ and -$(CH_3OH)_{n=1-3}$, the lowest frequency band shifts to the lower frequency side with the increase of the number of the solvent molecules. On the other hand, in BN-$(CHCl_3)_{n=1-3}$, the lowest frequency Raman band shifts to the higher frequency side with increase of the number of solvent molecules. These results are explained by the difference of the type of the cluster structure, that is "ring type" or "shell type", and a change of the flexibility of the clusters with the size.

The authors thank Drs. A. Fujii, H. Ishikawa, and T. Maeyama for helpful discussions. This work was partially supported by Grants-in-Aid for Scientific Research (No. 10440165) from the Ministry of Education, Science, Sports and Culture, Japan.

References

1. T. Ebata, A. Fujii, N. Mikami, Int. Rev. Phys. Chem. **17**, 331 (1998) and references therein
2. S. Ishikawa, T. Ebata, N. Mikami, J. Chem. Phys. **110**, 9504 (1999)
3. R. Yamamoto, S. Ishikawa, T. Ebata, N. Mikami, J. Raman Spectrosc. **31**, 295 (2000)
4. R. Yamamoto, T. Ebata, N. Mikami, J. Chem. Phys. **114**, 7866 (2001)
5. J.W. Nibler, G.A. Pubanz, in *Advances in non-linear spectroscopy*, edited by R.J.H. Clark, R.E. Hester (Wiley, New York, 1988), p. 1
6. H.D. Barth, F. Huisken, Chem. Phys. Lett. **169**, 169 (1990)
7. P.M. Felker, P.M. Maxton, M.W. Schaeffer, Chem. Rev. **94**, 1787 (1994) and references therein
8. P.M. Maxton, M.W. Schaeffer, S.M. Ohline, W. Kim, V.A. Venturo, P.M. Felker, J. Chem. Phys. **101**, 8391 (1994)
9. P.M. Maxton, M.W. Schaeffer, P.M. Felker, Chem. Phys. Lett. **241**, 603 (1995)
10. W. Kim, P.M. Felker, J. Chem. Phys. **108**, 6763 (1998)
11. W. Kim, M.W. Schaeffer, S. Lee, J.S. Chung, P.M. Felker, J. Chem. Phys. **110**, 11264 (1999)
12. W. Kim, S. Lee, P.M. Felker, J. Chem. Phys. **112**, 4527 (2000)
13. R.M. Helm, H.-P. Vogel, H.J. Neusser, Z. Naturforsch. **52a**, 655 (1997)
14. V. Storm, H. Dreizler, D. Consalvo, Chem. Phys. **239**, 109 (1998)
15. S. Melandri, D. Consalvo, W. Caminati, P.G. Favero, J. Chem. Phys. **111**, 3874 (1999)
16. T. Kobayashi, K. Honma, O. Kajimoto, S. Tsuchiya, J. Chem. Phys. **86**, 1111 (1987)
17. T. Kobayashi, O. Kajimoto, J. Chem. Phys. **86**, 1118 (1987)
18. K. Sakota, K. Nishi, K. Ohashi, H. Sekiya, Chem. Lett. 618 (2000)
19. M.J. Frisch *et al.*, *Gaussian 98*, Revision A.7, Gaussian, Inc., Pittsburgh PA, 1998
20. T.S. Zwier, Annu. Rev. Phys. Chem. **47**, 205 (1996); and references therein
21. Y. Tsutui, H. Wasada, Chem. Lett. 517 (1995)